Asynchronous field-induced ferromagnetism of the two Fe sub-lattices in (Hf,Ta)Fe_2: Emergence of an additional first-order phase transition

Cite as: APL Mater. 13, 031112 (2025); doi: 10.1063/5.0248935
Submitted: 14 November 2024 • Accepted: 26 February 2025 •
Published Online: 19 March 2025

Tapas Samanta,[1,a)] Sven Wiesekopsieker,[1] Chris Taake,[1] and Luana Caron[1,2]

AFFILIATIONS

[1] Faculty of Physics, Bielefeld University, P.O. Box 100131, D-33501 Bielefeld, Germany
[2] Helmholtz-Zentrum Berlin für Materialien und Energie, Berlin 12489, Germany

[a)] **Author to whom correspondence should be addressed:** tapas.sinp@gmail.com and tsamanta@physik.uni-bielefeld.de

ABSTRACT

The field-induced change of the magnetic phase transitions in partially Ta-substituted $Hf_{0.84}Ta_{0.16}Fe_2$ has been examined by combining dc-magnetization, ac-susceptibility, magnetoresistance, and analysis of the isothermal entropy change [$\Delta S \propto (\mu_0 H)^n$] field-exponent ($n$). The system exhibits a first-order magnetic transition (FOMT) from a ferromagnetic (FM) to an antiferromagnetic (AFM) state at T_C (262 K) and a second-order AFM to paramagnetic (PM) transition at T_N (323 K) for lower applied field $\mu_0 H$ = 0.1 T. The shift of T_C and T_N follows opposite trends with increasing $\mu_0 H$ as expected for this material class. However, a field-induced FOMT has been observed associated with T_N above 2 T, as confirmed by the negative slope of the inverse Arrott plot, the phase transition peak in ac-susceptibility, a slope change in isothermal magnetoresistance, and an overshoot of n greater than 2. The result can be ascribed to the asynchronous field-induced FM ordering of adjacent antiferromagnetically coupled 6h Fe sub-lattices at T_N, which results in the increase of the temperature range of the FOMT.

I. INTRODUCTION

The interlayer and intralayer magnetic interactions of the two interpenetrating Fe-sub-lattices (2a and 6h sites of the hexagonal C14 structure) in Laves phase $Hf_{1-x}Ta_xFe_2$ compounds can result in either FM or AFM ground states depending on the Hf:Ta ratio.[1,2] The Hf-rich compound is FM, whereas the Ta-rich compound stabilizes in the AFM state.[3,4] In the composition range $0.1 < x < 0.25$, the AFM state is metastable, which results in a FOMT from the AFM to the FM state at T_C upon cooling.[2,5,6] A second-order magnetic transition, at T_N (AFM–PM), has been observed at higher temperature. It has been revealed from earlier Mössbauer spectroscopy and neutron diffraction studies that neighboring 6h Fe sub-lattices are antiferromagnetically coupled in the AFM state.[4,5] The exchange field produced by antiferromagnetically coupled 6h Fe sub-lattices creates frustration on the 2a Fe sub-lattice due to the inversion symmetry of the hexagonal crystal structure and prohibits magnetic ordering of the 2a Fe sub-lattice until FM ordering is established for the 6h Fe sites.[4–6] Both 6h and 2a sub-lattices order ferromagnetically at T_C.[4–6] The first-order AFM–FM transition at T_C can be established either by changing the temperature or applying a magnetic field. The temperature-induced FOMT is associated with an isostructural phase transition from the lower-volume AFM to the higher-volume FM state, which has the potential to exhibit technologically important large negative thermal expansion (NTE) properties.[6–8] The field-induced FOMT resulting from the itinerant electron metamagnetism (IEM) is beneficial for large magnetocaloric (MCE) properties that can be utilized in magnetic cooling applications.[9,10] The FOMT is also responsible for large magnetoresistance properties.[11–13] Therefore, $Hf_{1-x}Ta_xFe_2$ is a promising class of materials exhibiting multifunctional properties associated with the temperature- or field-induced modification of the FOMT at T_C.

The second-order magnetic transition at T_N has negligible influence on the functional properties.

Earlier studies indicate that the magnetic properties of $Hf_{1-x}Ta_xFe_2$ exhibit an itinerant-electron character.[3,14] The qualitative behavior of the phase transitions (at T_C and T_N) and the associated magnetic phase diagram of $Hf_{1-x}Ta_xFe_2$ can be described by the Moriya–Usami (M–U) model for itinerant-electron systems with $T_N > T_C$, considering the spin fluctuations of coexisting AFM and FM phases.[3,14,15] According to this model,[15] the critical field-value ($\mu_0 H_C$) of the field-induced phase transition increases with increasing temperature for the FM–AFM transition (at T_C) and increases with decreasing temperature for the AFM–PM transition (at T_N). The first- and second-order (at T_C and T_N, respectively) phase transitions merge at a certain critical field (maximum field value to realize a field-induced transition) and temperature (which lies between T_C and T_N). The overall ($\mu_0 H$, T) phase boundary takes a semicircular form where part of the phase transition is first-order in nature and the remaining part is characterized as second-order. In the literature, the magnetic phase transitions of $Hf_{1-x}Ta_xFe_2$ are usually described based on the M-U model. According to the M-U model, the range of the FOMT associated with T_C (which is responsible for the functional properties) is restricted by the evolution of the second-order magnetic transition at T_N. For systems having an AFM ground state (instead of a metastable AFM state in the presently studied system), $\mu_0 H_C$ is observed to increase with decreasing temperature at the field-induced FOMT as observed in $Hf_{0.75}Ta_{0.25}Fe_2$ and in the hydrostatic-pressure induced study of $Hf_{0.825}Ta_{0.175}Fe_2$.[14,16] This is inconsistent with the M-U model. In those studies, the authors pointed out that the above-mentioned discrepancy can be explained by considering the magnetovolume coupling, which is not taken into account in the free energy expression of the M-U model. An asynchronous FM ordering of Fe moments at 6*h* and 2*a* sub-lattices as revealed by electron spin resonance results in a large NTE window for (Hf,Ta)Fe_2 associated with spontaneous volume magnetostriction (SVM) in both Fe 2*a* and 6*h* sub-lattices depending on their respective temperature and field dependence.[7] The above-mentioned observation indicates that a field-induced destabilization of the AFM state could result in a FOMT at T_N and, therefore, broaden the temperature range in which functional properties could be achieved. This motivated us to examine the order of the phase transition associated with T_N in $Hf_{0.84}Ta_{0.16}Fe_2$. We have observed a field-induced FOMT at T_N for $Hf_{0.84}Ta_{0.16}Fe_2$, as evident from different experimental results, which is the direct consequence of the asynchronous field-induced FM ordering of adjacent 6*h* Fe sub-lattices. The FOMT at T_N results in an effective increase of the temperature range of the FOMT when combined with the FOMT at T_C.

II. EXPERIMENTAL

A polycrystalline $Hf_{0.84}Ta_{0.16}Fe_2$ sample was produced by arc melting of the constituent elements of purity better than 99.9% under an ultra-high purity Ar atmosphere. Room-temperature powder X-ray diffraction (XRD) measurements of the samples were carried out in a Philips X'Pert Pro MPD diffractometer using Cu K_α radiation. The structural refinement of the XRD data was performed using the FullProf software.[17] A Quantum Design MPMS 3 magnetometer was employed for dc-magnetization, ac-susceptibility, and magnetoresistance measurements. High-temperature magnetization measurements up to 750 K were performed using the oven option of the MPMS 3 magnetometer. To improve the accuracy in the estimation of the ΔS for a FOMT,[18] isofield $M(T)$ data have been measured for calculations using the Maxwell relation

$$\Delta S(T, \mu_0 H) = \sum_j \frac{M_{j+1}(T_{j+1}, \mu_0 H) - M_j(T_j, \mu_0 H)}{T_{j+1} - T_j} \Delta \mu_0 H,$$

where M_{j+1} (T_{j+1}, $\mu_0 H$) and M_j (T_j, $\mu_0 H$) are the values of magnetization in a magnetic field $\mu_0 H$ at temperatures T_{j+1} and T_j, respectively.

III. RESULTS AND DISCUSSION

The refinement of the room-temperature XRD pattern is shown in Fig. 1. A hexagonal C14 Laves phase structure (space group $P6_3/mmc$) has been observed, which is consistent with earlier reports for similar compositions.[8–11] The lattice parameters estimated from the Rietveld refinement of the XRD data were found to be a = 4.929(1) Å and c = 8.062(3) Å at room-temperature.

The temperature dependence of the dc magnetization (M) and corresponding inverse susceptibility ($1/\chi_{dc}$) for $\mu_0 H$ = 0.1 T is shown in Fig. 2(a). A sharp jump of the magnetization around T_C = 262 K is associated with a FOMT, which is consistent with the reported AFM–FM FOMT for the studied composition range.[2,6,9–12] A second phase transition is also clearly visible in the $1/\chi_{dc}(T)$ around 323 K, which is a typical second-order AFM–PM transition (T_N).[2,6,11,12] The FOMT at T_C and the second-order magnetic transition at T_N are observed in the temperature dependence of the real (χ') and imaginary (χ'') parts of the ac-susceptibility as shown in Figs. 2(b) and 2(c), respectively. The zero-field resistivity (ρ) as a function of temperature also shows a jump at T_C, indicating a FOMT [Fig. 2(d)].

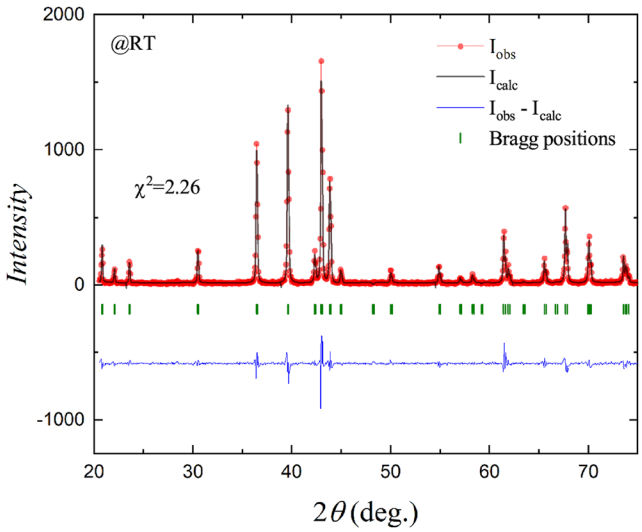

FIG. 1. Rietveld refinement profile of the room-temperature XRD data for $Hf_{0.84}Ta_{0.16}Fe_2$.

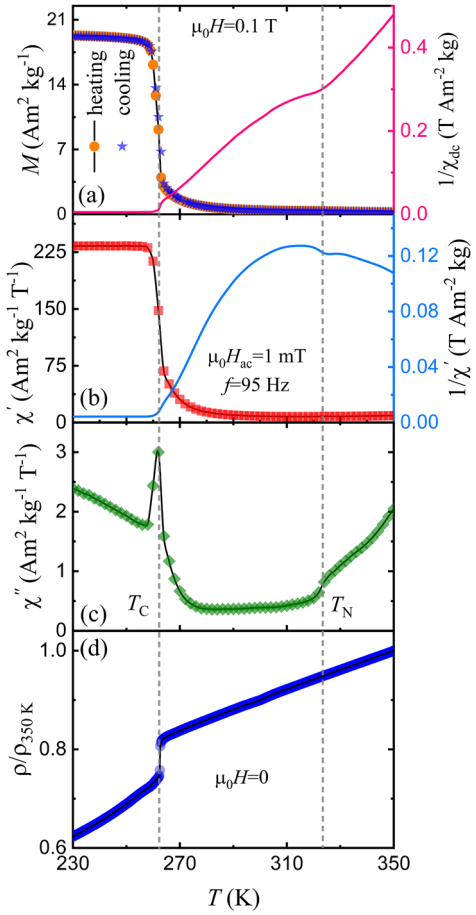

FIG. 2. (a) Temperature-dependent dc magnetization (M) during heating as well as cooling and associated inverse susceptibility with the application of $\mu_0 H$ = 0.1 T. (b) The real part of the ac-susceptibility (χ') and its inverse variation as a function of temperature. (c) The corresponding temperature dependence of the imaginary part (χ'') of the ac-susceptibility. (d) The zero-field resistivity (ρ) as a function of temperature. T_C and T_N represent the FOMT AFM–FM transition and the second-order AFM–PM magnetic transition, respectively.

At low field, the observed phase transitions are identical to those reported in the literature.[2,6,7,11,12]

The temperature dependence of the entropy change (ΔS) for a magnetic field change up to 7 T is shown in Fig. 3(a). A reasonably large negative ΔS has been observed, particularly for lower $\mu_0 H$ during cooling (equivalent to the change of ΔS due to the application of $\mu_0 H$) associated with the FOMT from AFM to FM state. The magnitude of the ΔS upon heating is similar to that of the cooling process but with an opposite sign. Due to the negligible thermal hysteresis of the magnetoelastic FOMT, a large reversible ΔS ($|\Delta S_{rev}|$ is estimated from the overlapping region of the temperature-dependent ΔS curves on heating and cooling) is observed. The maximum values of $|\Delta S_{rev}|$ were found to be 3.25 and 3.84 J/kg K for the field changes of $\mu_0 H$ = 1 and 2 T, respectively, which is comparable to the best reported values in this class of materials.[9,10] Another interesting point to be noted here is that a change of ΔS is also visible near T_N, which is associated with the field-induced modification of the magnetic ordering in the 6*h* Fe sub-lattices. In general, the change of ΔS around T_N is overlooked due to its lower magnitude. However, the FM ordering of the 2*a* Fe sub-lattices at T_C also depends on the nature of the magnetic ordering of the 6*h* Fe sub-lattices. As mentioned earlier, the FM ordering of the frustrated disordered 2*a* Fe sub-lattices can only be established if the magnetic ordering of the adjacent 6*h* Fe sub-lattices transforms from AFM to FM state.[4–6] Therefore, the transitions at T_C and T_N are both influenced by the nature of the magnetic ordering of adjacent 6*h* Fe sub-lattices. Based on this idea, the behavior of the transitions at T_N and T_C as a function of both magnetic field and temperature has been examined as follows.

In general, ΔS follows a power-law dependence with the magnetic field as $\Delta S \propto (\mu_0 H)^n$.[19,20] The local field exponent, n, can be estimated as[19,20]

$$n = \frac{dln|\Delta S|}{dln(\mu_0 H)}.$$

Law *et al.*[20] developed a quantitative criterion to identify the order of magnetic phase transitions based on the value of n^{max}. According to this criterion, $n^{max} > 2$ signifies a FOMT, whereas $n^{max} \leq 2$ is an indication of a second-order phase transition. This criterion has been successfully implemented to determine the order of the phase transition for different classes of materials.[20,21] The temperature dependence of n for different $\mu_0 H$ is shown in Fig. 3(b). For lower applied fields ($\mu_0 H$ = 0.5 T), n^{max} is well above 2 around T_C, indicating a FOMT associated with the simultaneous FM ordering of both 6*h* and 2*a* sub-lattices. However, there is no overshoot of n^{max} above 2 near T_N, confirming the second-order nature of the AFM–PM transition for $\mu_0 H$ = 0.5 T. For further increase of $\mu_0 H$ (≥1 T), a second peak starts to appear in the $n(T)$ curve near T_N with $n^{max} > 2$, resembling a FOMT associated with the field-induced FM ordering of antiferromagnetically coupled neighboring 6*h* Fe sub-lattices (the corresponding FOMT denoted as T_C^{6h}). The observed negative slope in the $\mu_0 H/M$ vs M^2 plot in the close vicinity of T_N [as shown in Fig. 3(c)] also confirms the first-order nature of the phase transition consistent with Banerjee's criterion for FOMT.[22] As is clear from the plot in Fig. 3(b), the peak position of the $n(T)$ curve associated with the FM–AFM transition taking place at T_C shifts toward higher temperatures with increasing $\mu_0 H$ (~3 T), whereas the corresponding peak related to the phase transition at T_C^{6h} moves in the opposite direction. Eventually the two peaks merge into a single peak for $\mu_0 H > 3$ T. For $\mu_0 H > 4$ T, a single n^{max} peak is observed, which progressively decreases due to the broadening of the phase transition with the application of the field. Most interestingly, n^{max} follows opposite trends for the transition at T_C (n^{max} decreases) and T_C^{6h} (n^{max} increases) with increasing $\mu_0 H$ (up to about 3 T). This change of n^{max} indicates that the field-induced growth of the first-order character of the phase transition at T_C^{6h} makes the FOMT weaker at T_C. For lower applied $\mu_0 H$, the stronger FOMT at T_C is associated with a large negative magnetovolume effect (connected with negative thermal expansion) resulting from more compressed frustrated AFM 6*h* Fe sub-lattices.[6] When $\mu_0 H$ is sufficiently large so that an isolated field-induced FM ordering of the 6*h* Fe sub-lattices is possible at T_C^{6h}, then the concomitant field-induced positive magnetostriction of the AFM 6*h* Fe sub-lattices reduces the negative

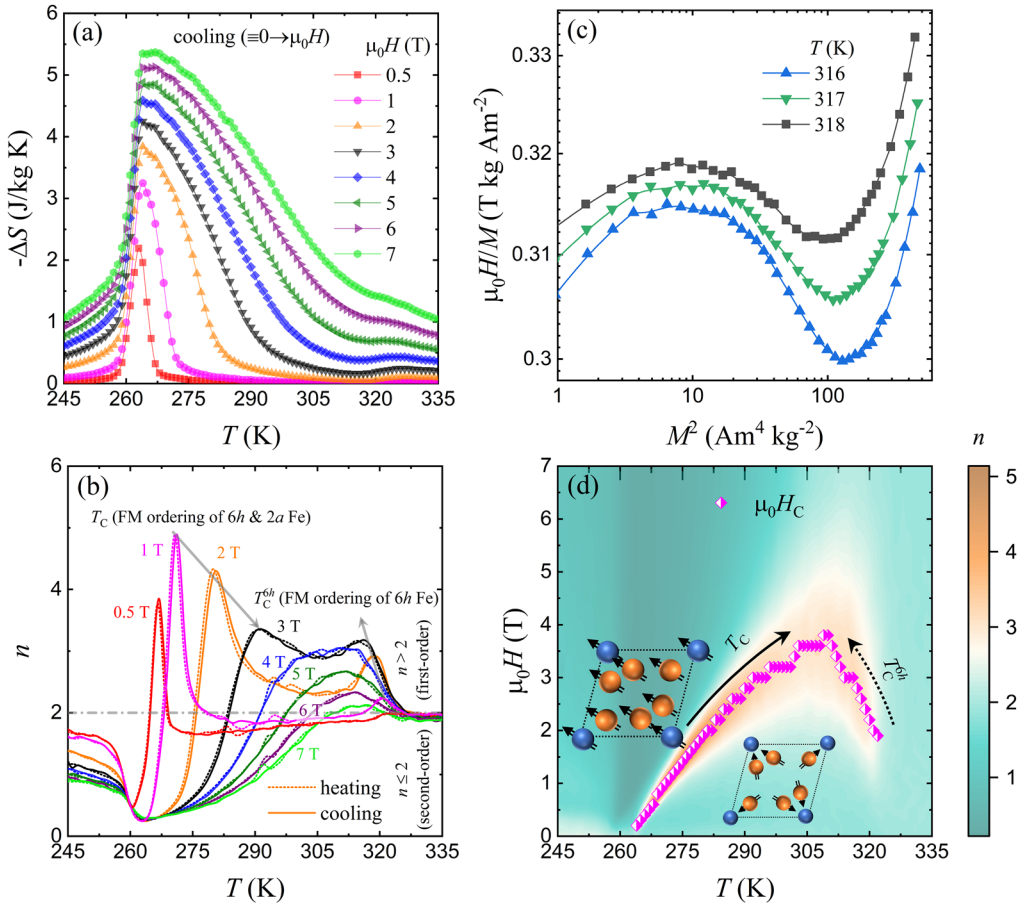

FIG. 3. (a) Temperature dependence of the isothermal entropy change (−ΔS) during cooling for a field change up to 7 T. (b) Temperature-dependence of the field-exponent n for different $\mu_0 H$. (c) Log–log $\mu_0 H/M$ vs M^2 plot in the close vicinity of T_N. (d) 2D color-contour plot of the variation of n as a function of temperature and magnetic field. The critical field value $\mu_0 H_C$ corresponding to n^{max} is shown by the diamond symbol. T_C^{6h} represents the FOMT associated with an asynchronous field-induced FM ordering of adjacent 6*h* Fe sub-lattices. Insets: The magnetic structures of AFM and FM states are shown along the crystallographic *c*-direction.

magnetovolume effect for the phase transition at T_C, making the FOMT weaker.[6]

The 2D color-contour plot of the variation of $n(T, \mu_0 H)$ is shown in Fig. 3(d). The temperature dependence of the critical field ($\mu_0 H_C$ to realize n^{max}, which is equivalent to the critical field value for the FOMT) shows a profile identical (a semicircular shape of the phase boundary) to that theoretically described by the Moriya–Usami model for itinerant-electron systems with $T_N > T_C$ [Fig. 3(b) in Ref. 15]. However, there is a significant difference in the order of the phase transition observed in the present study when compared with that described by the Moriya–Usami model. In particular, a substantial part of the AFM phase boundary (T_N) is first-order in nature (denoted as T_C^{6h}); however, the Moriya–Usami model predicts it as second order. The discrepancy possibly arises due to the asynchronous FM ordering of the Fe moments at the 6*h* and 2*a* sub-lattices and their respective SVM.[7,16] The schematic representation of the magnetic structures is shown in the insets of Fig. 3(d) for AFM and low-temperature FM states as conceptually adopted from Ref. 6.

The evolution of the critical field ($\mu_0 H_C$) for the FOMT is also examined using isothermal ac-susceptibility measurements by varying the dc-magnetic field. The field dependence of the real part of the ac-susceptibility (χ') is shown in Fig. 4. Interestingly, the temperature dependence of the magnetic field value $\mu_0 H$ corresponding to the peak in $\chi'(\mu_0 H)$ evolves in the same manner as observed in $\mu_0 H_C(T)$ to realize n^{max} [see Fig. 3(d)]. In particular, the observed peak in $\chi'(\mu_0 H)$ and temperature evolution of the corresponding $\mu_0 H$ associated with T_C^{6h} once again indicate an isolated field-induced first-order FM ordering of adjacent 6*h* Fe sub-lattices.

The phase transition characteristics of T_C and T_N were further examined through magnetotransport measurements. The isothermal magnetoresistance ($MR = \{\rho(\mu_0 H) - \rho(0)/\rho(0)\}$) as a function of $\mu_0 H$ is shown in Fig. 5(a). A negative *MR* has been observed with increasing $\mu_0 H$ in the studied temperature range, which is consistent with earlier studies.[11–13] The sharp decrease of *MR* for a narrow field range in the vicinity of T_C indicates an AFM–FM FOMT where field-induced FM ordering of both Fe 2*a* and 6*h* sub-lattices results in a large reduction of $\rho(\mu_0 H)$.[13] It is also clearly visible that the jump in

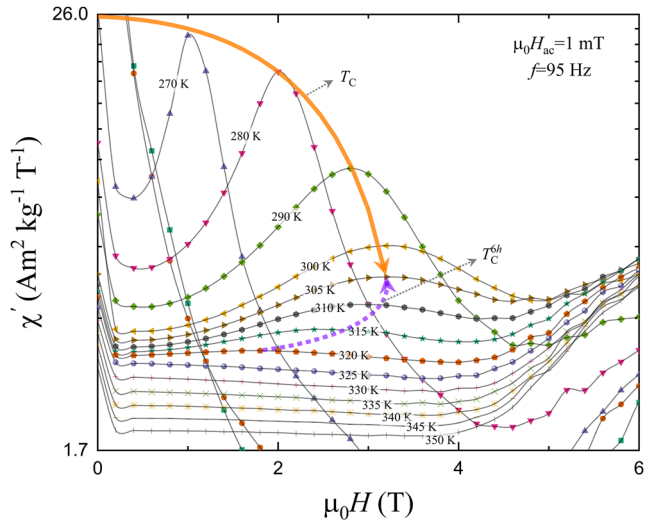

FIG. 4. Isothermal variation of the real part of ac-susceptibility (χ') as a function of the dc magnetic field $\mu_0 H$. The variations of T_C and T_C^{6h} are indicated by curved arrows.

MR (with decreasing magnitude) shifts to higher fields with increasing temperature up to about 285 K, indicating an enhancement of the critical field $\mu_0 H_C$ for the FOMT at T_C resulting from the simultaneous FM ordering of both Fe 2*a* and 6*h* sub-lattices. Above 285 K, the sharp change in MR associated with the field-induced FOMT is smeared out, and the saturation tendency after the field-induced phase transition almost disappears. However, a slope change can still be observed in a log–log $|MR|(\mu_0 H)$ up to about T_N [as shown in Figs. 5(b)–5(d)] and finally disappears in the PM state [as shown in Fig. 5(e)]. The observed slope change in $|MR|(\mu_0 H)$ below T_N indicates a field-induced FOMT transition because the phase transition occurs inside an AFM ordered state (i.e., an order-order phase transition, which is therefore intrinsically first order). The temperature dependent ρ measured by varying the $\mu_0 H$ from 0 to 7 T also exhibits a field-induced decrease of ρ below T_N [plotted in Fig. 5(f)]. The $\mu_0 H_C$ of the FOMT corresponds to the field value where the high-field $|MR|(\mu_0 H)$ starts to deviate from linearity. The maximum value of $\mu_0 H_C$(max) has been identified near 310 K, which is equivalent to that observed in $n(T, \mu_0 H)$ [as shown in Fig. 3(d)]. $\mu_0 H_C$ increases and decreases with increasing temperature below and above the maximum $\mu_0 H_C$, respectively. As already established for this class of materials, only the exchange interaction between adjacent 6*h* Fe sub-lattices is responsible for the AFM ordering below T_N while the 2*a* Fe sub-lattices remain disordered above T_C in the AFM state. The observed increase of $\mu_0 H_C$ with decreasing temperature down to $\mu_0 H_C$(max) is expected for AFM systems due to the reduction of thermal fluctuation, resembling a field-induced FM ordering of adjacent 6*h* Fe sub-lattices [the corresponding phase transition is indicated as T_C^{6h} in Fig. 3(d)]. A similar type of temperature dependence of $\mu_0 H_C$ has been reported earlier for (Hf,Ta)Fe_2, which has an AFM ground state.[14,16] The field-induced FOMT at T_N is a consequence of an asynchronous FM ordering of the Fe moments at the 6*h*

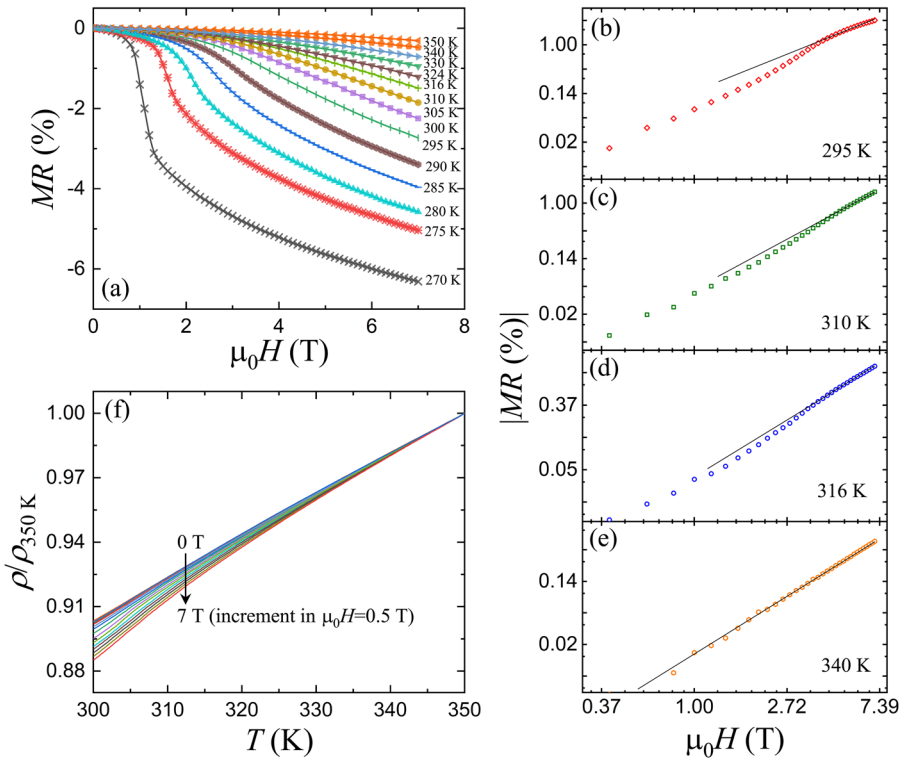

FIG. 5. (a) Isothermal magnetoresistance (*MR*) as a function of magnetic field. Log–log *MR* vs $\mu_0 H$ plot at (b) 295 K, (c) 310 K, (d) 316 K, and (e) 340 K. (f) Resistivity (ρ) as a function of temperature for $\mu_0 H$ = 0–7 T.

sub-lattices similar to that observed earlier for the (Hf,Ta)Fe_2 system using electron spin resonance.[7]

IV. CONCLUSION

In our present experimental study on the $Hf_{0.84}Ta_{0.16}Fe_2$ system, it has been observed that the phase boundaries associated with T_C and T_N evolve similarly as theoretically predicted in the M-U model for itinerant-electron systems; however, it deviates strikingly in what concerns the order of the phase transition at T_N, particularly for higher applied magnetic fields. A substantial part of the AFM phase boundary (T_N) is first-order in nature, in contrast with the M-U model that predicts it as second-order. The experimental results indicate that an asynchronous field-induced FM ordering of adjacent 6*h* Fe sub-lattices is responsible for the change of the transition order at T_N from second- to first-order. The observed FOMT at T_N could be useful for broadening the working temperature range for functional properties, such as NTE.

ACKNOWLEDGMENTS

This work was carried out in the framework of the Joint Lab BiBer and was supported by the BMBF joint project DiProMag—Digitalization of a process chain for the production, characterization, and prototypical application of magnetocaloric alloys, here the contribution of Bielefeld University: Grant No. FKZ 13XP5 120B, with the objective of producing magnetocaloric Heusler compounds and ontology development.

AUTHOR DECLARATIONS

Conflict of Interest

The authors have no conflicts to disclose.

Author Contributions

Tapas Samanta: Conceptualization (equal); Formal analysis (equal); Investigation (equal); Visualization (lead); Writing – original draft (lead); Writing – review & editing (lead). **Sven Wiesekopsieker**: Formal analysis (equal); Investigation (equal); Software (equal); Writing – review & editing (equal). **Chris Taake**: Formal analysis (equal); Investigation (equal); Software (lead); Writing – review & editing (equal). **Luana Caron**: Conceptualization (equal); Funding acquisition (lead); Resources (lead); Supervision (lead); Visualization (equal); Writing – original draft (equal); Writing – review & editing (equal).

DATA AVAILABILITY

The data that support the findings of this study are available from the corresponding author upon reasonable request.

REFERENCES

[1] L. V. B. Diop, D. Benea, S. Mankovsky, and O. Isnard, J. Alloys Compd. **643**, 239 (2015).
[2] H. Wada, N. Shimamura, and M. Shiga, Phys. Rev. B **48**, 10221 (1993).
[3] Y. Nishihara and Y. Yamaguch, J. Phys. Soc. Jpn. **52**, 3630 (1983).
[4] L. V. B. Diop, O. Isnard, E. Suard, and D. Benea, Solid State Commun. **229**, 16 (2016).
[5] H. R. Rechenberg, L. Morellon, P. A. Algarabel, and M. R. Ibarra, Phys. Rev. B **71**, 104412 (2005).
[6] B. Li, X. H. Luo, H. Wang, W. J. Ren, S. Yano, C. W. Wang, J. S. Gardner, K.-D. Liss, P. Miao, S. H. Lee, T. Kamiyama, R. Q. Wu, Y. Kawakita, and Z. D. Zhang, Phys. Rev. B **93**, 224405 (2016).
[7] L. F. Li, P. Tong, Y. M. Zou, W. Tong, W. B. Jiang, Y. Jiang, X. K. Zhang, J. C. Lin, M. Wang, C. Yang, X. B. Zhu, W. H. Song, and Y. P. Sun, Acta Mater. **161**, 258 (2018).
[8] Q. Shen, F. Zhang, I. Dugulan, N. van Dijk, and E. Brück, Scr. Mater. **232**, 115482 (2023).
[9] F. -H. Chen, H. -B. Xie, M. -S. Huo, H. Wu, L. -J. Li, and Z. -Y. Jiang, Tungsten **5**, 503 (2023).
[10] Z. Song, Z. Li, B. Yang, H. Yan, C. Esling, X. Zhao, and L. Zuo, Materials **14**, 5233 (2021).
[11] Y. Nagata, T. Hagii, S. Yashiro, H. Samata, and S. Abe, J. Alloys Compd. **292**, 11 (1999).
[12] L. V. B. Diop, J. Kastil, O. Isnard, Z. Arnold, and J. Kamarad, J. Appl. Phys. **116**, 163907 (2014).
[13] H. G. M. Duijn, *Magnetotransport and Magnetocaloric Effects in Intermetallic Compounds* (Van der Waals-Zeeman Institute, 2000).
[14] H. Nishihara, G. Kido, Y. Nishihara, M. Itoh, and H. Yasuoka, Solid State Commun. **49**, 1113 (1984).
[15] T. Moriya and K. Usami, Solid State Commun. **23**, 935 (1977).
[16] L. V. B. Diop, O. Prokhnenko, O. Isnard, G. Ballon, and J. P. Itié, Intermetallics **129**, 107054 (2021).
[17] J. Rodríguez-Carvajal, *Introduction to the Program FULLPROF: Refinement of Crystal and Magnetic Structures from Powder and Single Crystal Data* (Laboratoire Léon Brillouin, CEA Saclay, 2015).
[18] L. Caron, N. B. Doan, and L. Ranno, J. Phys.: Condens. Matter **29**, 075401 (2017).
[19] T. D. Shen, R. B. Schwarz, J. Y. Coulter, and J. D. Thompson, J. Appl. Phys. **91**, 5240 (2002).
[20] J. Y. Law, V. Franco, L. M. Moreno-Ramírez, A. Conde, D. Y. Karpenkov, I. Radulov, K. P. Skokov, and O. Gutfleisch, Nat. Commun. **9**, 2680 (2018).
[21] C. Taake, T. Samanta, and L. Caron, Appl. Phys. Lett. **124**, 052403 (2024).
[22] B. K. Banerjee, Phys. Lett. **12**, 16 (1964).